Neuroscience Vol. 55, No. 2, pp. 339–351, 1993
Printed in Great Britain

0306-4522/93 $6.00 + 0.00
Pergamon Press Ltd

EXTRACELLULAR SPACE PARAMETERS IN THE RAT NEOCORTEX AND SUBCORTICAL WHITE MATTER DURING POSTNATAL DEVELOPMENT DETERMINED BY DIFFUSION ANALYSIS

A. LEHMENKÜHLER,* E. SYKOVÁ,†‡ J. SVOBODA,† K. ZILLES§ and C. NICHOLSON‖

*Institute of Physiology, University of Münster, Robert-Koch-Str. 27a, 4400 Münster, Germany
†Laboratory of Cellular Neurophysiology, Institute of Experimental Medicine AV CR, Bulovka, Pavilon 11, 180 85 Prague 8, Czech Republic
§C.u O. Vogt-Institute for Brain Research, Heinrich Heine University, Düsseldorf, Germany
‖Department of Physiology and Biophysics, New York University Medical Center, NY 10016, U.S.A.

Abstract—Extracellular space volume fraction, tortuosity and nonspecific uptake of tetramethylammonium—three diffusion parameters of brain tissue—were measured in gray matter of the somatosensory neocortex and subcortical white matter of the rat during postnatal development. The three parameters were determined from concentration–time profiles of tetramethylammonium in postnatal days 2–120 *in vivo*. Tetramethylammonium concentration was measured with ion-selective microelectrodes positioned 130–200 μm from an iontophoretic source. Data were correlated with cytoarchitectonic structure and average thickness of the regions in 0–90-day-old rats using rapidly frozen tissue.

Extracellular space volume fraction was largest in the newborn rats and diminished with age. In two- to three-day-old animals, volume fraction (mean ± S.E.) was 0.36 ± 0.04 in layers III and IV, 0.38 ± 0.02 in layer V, 0.41 ± 0.01 in layer VI and 0.46 ± 0.01 in white matter. The earliest decrease in volume fraction was found in layers V and VI at postnatal days 6–7 followed by a decrease in layer III and IV at postnatal days 8–9 and in white matter at postnatal days 10–11. A further dramatic reduction in volume fraction occurred in all cortical layers and especially in the white matter between postnatal days 10 and 21. There was no further decrease in volume fraction between postnatal day 21 and adults (90–120 days old). The adult volume fraction values were: layer II, 0.19 ± 0.002; III, 0.20 ± 0.004; IV, 0.21 ± 0.003; V, 0.22 ± 0.003; VI, 0.23 ± 0.007; white matter, 0.20 ± 0.008. Values of tortuosity ranged between 1.51 and 1.65, nonspecific cellular uptake varied from 3.3×10^{-3}/s to 6.3×10^{-3}/s. The variations in each parameter were not statistically significant at any age.

These data represent the first characterization of diffusion parameters in a developing brain. They confirm previous histological indications of a relatively large extracellular volume fraction during early postnatal development. The constancy of the tortuosity shows that diffusion of small molecules is no more hindered in the developing brain than in the adult. The large extracellular space volume fraction of the neonatal brain could significantly dilute ions, metabolites and neuroactive substances released from cells, relative to release in adults, and may be a factor in preventing anoxia, seizure and spreading depression in young animals. The diffusion characteristics could also play an important role in the developmental process itself.

Extracellular space (ECS) constitutes the microenvironment of brain cells. Its ionic composition, and the distribution of neurotransmitters, neuromodulatory compounds and metabolic substrates change dynamically during neuronal activity and can substantially affect the transmission of information in the nervous tissue. Therefore, ECS is an important communication channel between neurons, and between neurons and glial cells.[34,40,56,57] The diffusion parameters of the ECS affect the activity-related accumulation of substances in the ECS, their movement towards the adjacent neurons and glial cells and access of neurohormones released from axons (e.g. pituitary hormones) to the capillaries. Changes in ECS diffusion parameters can therefore profoundly influence intercellular signal transmission, susceptibility of the nervous tissue to anoxia and seizures and could be an important factor in manifestation of CNS diseases.[40,56,57]

The fundamental constraints for the diffusion of substances through the ECS are the ECS volume fraction (α; the restricted volume of the nervous tissue which is available for diffusion of substances), and ECS tortuosity (λ; increased path length for the diffusing particles between two points due to various obstacles, e.g. cellular membranes, and possibly long-chain glycoproteins and fixed charges).[37] In addition to α and λ the diffusion of substances towards the other cells can be affected by nonspecific, concentration-dependent cellular uptake (k').[35–37]

The diffusion parameters of the ECS and their dynamic changes can be studied *in vivo* as well as *in vitro* by the real-time iontophoretic method, which

‡To whom correspondence should be addressed.
Abbreviations: ECS, extracellular space; HL, hindlimb area; k', nonspecific cellular uptake; TMA, tetramethylammonium; α, volume fraction; λ, tortuosity.

uses ion-selective microelectrodes to follow the diffusion of an extracellular marker (e.g. the tetramethylammonium ion, TMA^+) applied by iontophoresis.[35,37,39] Typical values of α and λ (mean $\pm$ S.E.) found in rat cerebellum *in vivo* were $\alpha = 0.21 \pm 0.02$ and $\lambda = 1.55 \pm 0.05$,[37] and in spinal cord dorsal horn $\alpha = 0.24 \pm 0.01$, $\lambda = 1.54 \pm 0.04$.[53] *In vitro* the diffusion properties were not found to be significantly different in slices of the rat neostriatum,[47] while the lower α values, ranging between 0.12 and 0.18, have been found in slices of the rat hippocampus[32] as well as in cerebellar slices of guinea-pig.[23] The diffusion parameters were significantly altered in slices of the rat neostriatum by hypoxia,[47] in the rat spinal cord *in vivo* by ischemia[60] and in response to the electrical or nociceptive stimulation of a peripheral input,[53] and in slices of the rat hippocampus by an increase of potassium concentration in the perfusion solution.[32] Relative shrinkage of the ECS as a result of neuronal activity or of pathological states has been described in the CNS in various studies, and it has been proposed that it may influence synaptic transmission, intercellular communication, mental functions and concentration of neurohormones in peripheral blood.[2,13,14,19,45,50,53,55-57,64]

The diffusion properties of the developing brain have not yet been studied. A morphometric analysis in brains of developing animals revealed that the intercellular clefts are often wider than in adult animals.[43] The fractional volume of the ECS was found to be significantly larger in immature animals and it progressively decreased with age.[9,12,43,52,61,66] In the present study we analysed diffusion properties of the ECS in rat sensorimotor cortex during postnatal development using the real-time iontophoretic method developed by Nicholson and Phillips.[37] We have estimated α and λ for the ECS, as well as nonspecific TMA^+ uptake, in rats of two to 120 days old. TMA^+ diffusion profiles were analysed in control medium (agar), in individual cortical layers and in subcortical white matter. Some of these findings have previously appeared in abstract form.[29,54]

EXPERIMENTAL PROCEDURES

Physiological measurements

Experiments were performed on 48 rat pups (Wistar, Velaz Breeding Center, Prague) two to 21 days old, and on 12 rats 90–120 days old (250–350 g) which were regarded as adults. Animals were anaesthetized with urethane (1.6 g/kg i.p.) and placed in a rat head-holder. The body temperature

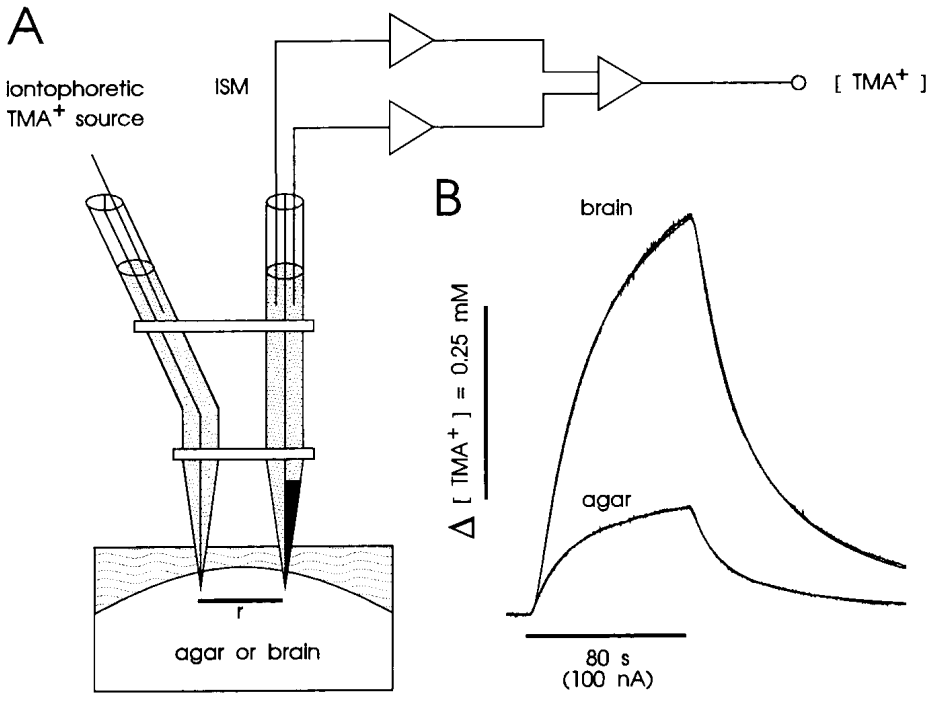

Fig. 1. Experimental set-up. A shows TMA^+-selective double-barrelled ion-sensitivie microelectrodes (ISM) fabricated from theta-capillary glass glued to a bent iontophoresis microelectrode, also made from theta-capillary. The separation between electrode tips was 150–200 μm. The ion-sensitive microelectrode was connected to a pair of high-impedance buffer amplifiers followed by a subtraction amplifier and connected to a digital oscilloscope and computer, as described in Experimental Procedures. B shows typical records obtained with this set-up. In this figure, and all subsequent ones, the concentration scale is linear and the theoretical diffusion curve (Eqn 1) is superimposed on each data curve. Measurements in agar gel where $\alpha = 1$ and $\lambda = 1$, enabled the transport number of the iontophoretic electrode to be determined as 0.37. When the electrode array was moved to the cortex, and the same iontophoretic main current applied, the resulting increase in concentration was much larger than that in agar due to the restricted α (0.38) and increased λ (1.52). The separation between electrode tips was 164 μm and the array was lowered 700 μm into the cortex of a three-day-old rat.

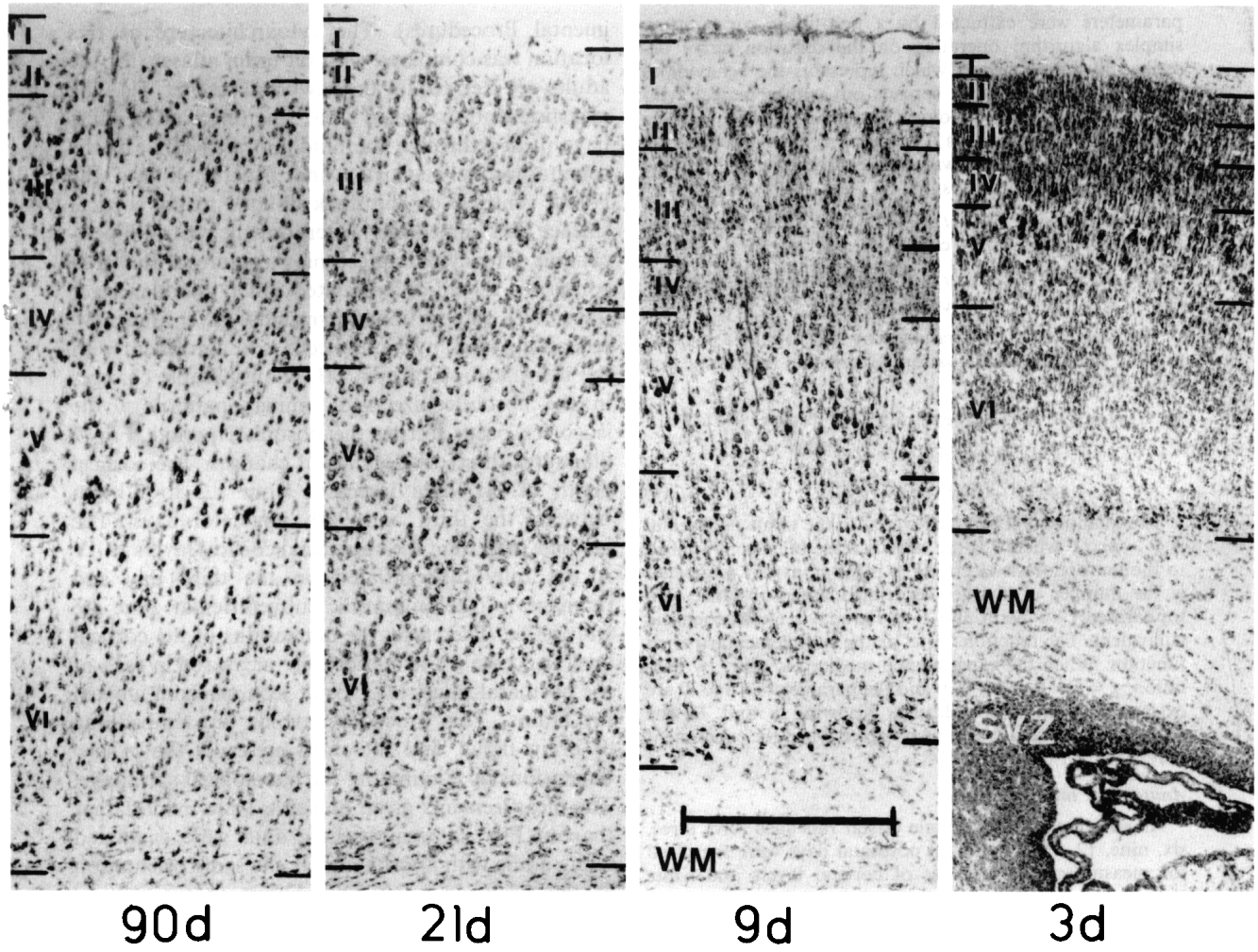

Fig. 2. Development of the cortical layers I–VI between postnatal days 3 and 90 in the rat hindlimb area. The laminar pattern of the most superficial cortical layers is not completely differentiated at the third postnatal day; the subventricular zone is still visible in this stage. All figures (Nissl stain) are vertically oriented to the cortical surface. The position of the hindlimb area in the dorsolateral isocortex leads to an electrode track, which is oblique to this direction. SVZ subventricular zone, WM white matter. Scale bar = 500 μm.

was maintained at 36–37°C by supporting the rat on a heated, curved platform that enclosed the lower part of the body. The animals spontaneously breathed air. A hole, 2.5 mm in diameter, was made over the somatosensory neocortex in the hind limb area and the dura carefully removed. The exposed brain tissue was bathed in warmed (36–37°C) artificial cerebrospinal fluid.[37]

Ion-sensitive microelectrodes for TMA^+ were made from double-barrelled theta glass tubing (Kuglstatter, Garching, F.R.G.) as described elsewhere.[39] The ion exchanger was Corning 477317 and the ion-sensing barrel was back-filled with 100 mM TMA chloride while the reference barrel contained 150 mM NaCl. Electrodes were calibrated using the fixed-interference method before and after each experiment in a sequence of flowing solutions of 150 mM NaCl + 3 mM KCl with the addition of the following amounts of TMA chloride (mM): 0.0003, 0.001, 0.003, 0.01, 0.03, 0.1, 0.3, 1.0, 3.0, 10.0. Calibration data were fitted to the Nikolsky equation to determine electrode slope and interference.[39]

For TMA^+ diffusion measurements, iontophoresis pipettes were prepared from theta glass. The shank was bent, before back-filling with 1 M TMA chloride, so that it could be aligned parallel to that of the ISM. Electrode arrays were made by gluing together an iontophoresis pipette and a TMA^+-ion-sensitive microelectrode with tip separation of 130–200 μm (Fig. 1). Typical iontophoresis parameters were +20 nA bias current (continuously applied to maintain a constant transport number), with +100 nA current step of 80 s duration to generate the diffusion curve.

Potentials recorded at the reference barrel of the ion-sensitive microelectrode were subtracted from ion-selective barrel voltage measurements by means of buffer and subtraction amplifiers (Fig. 1). TMA^+ diffusion curves were captured on a digital oscilloscope (Nicolet 3091), then transferred to a PC-compatible, 486 computer where they were analysed by fitting the data to a solution of the diffusion equation[37] (see below) using the program VOLTORO.

TMA^+ concentration vs time curves were first recorded in 0.3% agar gel (Difco, Special Noble Agar) made up in 150 mM NaCl, 3 mM KCl and 0.3 mM TMA^+ in a Lucite cup that could be placed just above the brain. The array of electrodes was then lowered into the cortex to appropriate depths to coincide with the known distribution of the layers at the various ages used, as defined by anatomical measurements (see below) summarized in Fig. 2.

The diffusion curves obtained from the various layers of the cortex were analysed to yield α and λ and the nonspecific, concentration-dependent uptake term, k' (s^{-1}). These three

parameters were extracted by a non-linear curve fitting simplex algorithm operating on the diffusion curve described by Eqn 1 below, which represents the behavior of TMA^+, assuming that it spreads out with spherical symmetry, when the iontophoresis current is applied for duration S. In this expression C is the concentration of the ion at time t and distance r away. The expression governing the diffusion in brain tissue is:

$C = G(t)$ $t < S$, for the rising phase of the curve.

$C = G(t) - G(t - S)$ $t > S$, for the falling phase of the curve.

The function $G(u)$ is evaluated by substituting t or $t - S$ for u in the following equation (Expression A14,[37] see also Refs 35, 36):

$$G(u) = (Q\lambda^2/8\pi D\alpha r)\{\exp[r\lambda(k'/D)^{1/2}]\,\mathrm{erfc}[r\lambda/2(Du)^{1/2} + (k'u)^{1/2}] + \exp[-r\lambda(k'/D)^{1/2} \times \mathrm{erfc}[r\lambda/2(Du)^{1/2} - (k'u)^{1/2}]\} \quad (1)$$

The quantity of TMA^+ delivered to the tissue per second is $Q = In/zF$ where I is the step increase in current applied to the iontophoresis electrode, n is the transport number, z is the number of charges associated with substance iontophoresed (+1 here) and F is Faraday's electrochemical equivalent. The function "erfc" is the complementary error function. When the experimental medium is agar, by definition, $\alpha = 1 = \lambda$ and $k' = 0$ and the parameters n and D are extracted by the curve fitting. Knowing n and D, the parameters α, λ and k' can be obtained when the experiment is repeated in the brain.

Anatomical measurements

An additional series of male Wistar rats aged zero, three, six, nine, 12, 15, 21, and 90 postnatal days were sacrificed for measuring the thickness of cortical layers and white matter along an orientation that corresponded to the way in which the ion-sensitive microelectrode array traversed the cortex. Immediately after decapitation the unfixed brains were removed and rapidly frozen in −70°C isopentane. Serial sectioning of these brains was performed with a cryostat microtome in the coronal plane. The use of unfixed, frozen brains was necessary to avoid the tissue shrinkage that is inevitable in fixed, paraffin-embedded tissue. The sections were mounted on gelatin-coated glass slides. The cell bodies were stained according to the method of Merker.[33] Sections were selected with the same rostrocaudal position (in adult animals an interaural position of 5.7–6.7 mm; bregma −2.3 to −3.3 mm, according to Zilles[69]) as used in the brains where the electrode recordings were made. In these sections the thicknesses of the different cortical layers and the white matter were measured microscopically along a line representing the electrode track, i.e. parallel to and about 3 mm lateral from the midsagittal plane. Layers II–IV were difficult to delineate as separate laminae during the first three postnatal days, because migration of neurones into these layers is still going on during that period. These layers, therefore, could not be measured separately at postnatal days 0–3 (see Fig. 2).

Statistical analysis

Results of the experiments were expressed as the mean ± S.E.M. Statistical analysis of the differences between groups was evaluated by one-way ANOVA test. Values of $P < 0.05$ were considered significant.

RESULTS

Morphological identification of layers in developing rat cortex

The location of the electrode penetration was identified in selected histological sections (see Experimental Procedures). The cytoarchitecture at this location was compared with rat brain atlases (for the adults, see Ref. 69; for the newborn, see Ref. 41). The measurements revealed that the electrodes must have passed through the hindlimb area (HL) of the somatosensory neocortex and penetrated into the lateral ventricle on the track oblique to the cortical surface and immediately lateral of the rostral hippocampus. The cytoarchitectonic structure of this area comprises a well-differentiated inner granular layer (layer IV) and an inner pyramidal layer (layer V) containing large pyramidal cells is in agreement with the identification of area HL. Considerable changes in the absolute size and laminar pattern of the isocortex occur during the postnatal period; Fig. 2 illustrates these developmental changes. The cortical depth of HL area increases from 1.2 to 2.1 mm between the third and 90th postnatal days. The laminar pattern of the superficial cortical layers II–IV is not fully differentiated on the third day and remnants of the embryonic subventricular zone are still visible. Therefore, the dimensions of the cortical layers and the white matter were measured in each of the postnatal stages in cryostat sections from unfixed rat brains. This procedure avoids any embedding of brain tissue, and therefore preserves the *in vivo* dimensions by eliminating the histological shrinkage. The measurements given in Table 1 are much larger than in Fig. 2, because these data were evaluated along a line with approximately the same orientation as the electrode track, i.e. oblique to the vertical orientation shown in Fig. 2. The average thicknesses of the cortical layers and white matter of rats aged zero, three, six, nine, 12, 15, 21 and 90 postnatal days ($n = 3$ of each) along the electrode track oblique to the cortical surface is shown in Fig. 3.

Diffusion parameters of the gray and white matter

The diffusion curves in somatosensory cortex were recorded with the tips of the microelectrode array aligned in longitudinal, orientation towards the sutura sagittalis. Both the rise and decay of each TMA^+ diffusion curve recorded in cortical layers II–VI and in subcortical white matter were well fitted by the diffusion equation solution (Eqn 1) irrespective of the age of animal (Fig. 4). We were not able to obtain a good fit of the TMA^+ diffusion curves in cortical layer I of the adult rats, and in cortical layers I and II of two- to 11-day-old rats, since the curves were not stable, apparently because the thickness of these layers is only 50–180 μm and the inter-tip distance of the electrodes was 130–200 μm; also in some animals the cortical surface might have been slightly damaged during opening of the skull and removal of dura mater. In layers III to VI and in the subcortical white matter, α was significantly higher in first postnatal days than in adult rats (Table 1). As can be seen from Table 1 in two- to three-day-old rats, the ECS volume fraction in the gray as well as in white matter is about double the ECS volume fraction in

Table 1. Extracellular space diffusion parameters as a function of age in postnatal days and cortical layers or subcortical white matter

Age in days	Cortical layer II	III	IV	V	VI	White matter
2–3	No data available	$\alpha = 0.36 \pm 0.035$ $\lambda = 1.65 \pm 0.048$ $k' = 5.1 \pm 1.1 \times 10^{-3}$/s $n = 8$ $d = 300\ \mu m$		$a = 0.38 \pm 0.020$ $\lambda = 1.68 \pm 0.026$ $k' = 6.7 \pm 1.6 \times 10^{-3}$/s $n = 12$ $d = 500\ \mu m$	$\alpha = 0.41 \pm 0.010$ $\lambda = 1.59 \pm 0.018$ $k' = 6.3 \pm 1.3 \times 10^{-3}$/s $n = 11$ $d = 700\ \mu m$	$\alpha = 0.46 \pm 0.014$ $\lambda = 1.58 \pm 0.054$ $k' = 7.5 \pm 3.3 \times 10^{-3}$/s $n = 6$ $d = 1100\ \mu m$
4–5	No data available	$\alpha = 0.32 \pm 0.022$ $\lambda = 1.62 \pm 0.045$ $k' = 2.9 \pm 0.6 \times 10^{-3}$/s $n = 8$ $d = 300\ \mu m$	$\alpha = 0.32 \pm 0.009$ $\lambda = 1.64 \pm 0.050$ $k' = 4.3 \pm 1.1 \times 10^{-3}$/s $n = 11$ $d = 500\ \mu m$	$\alpha = 0.35 \pm 0.019$ $\lambda = 1.66 \pm 0.031$ $k' = 4.2 \pm 0.4 \times 10^{-3}$/s $n = 24$ $d = 700, 900\ \mu m$	$\alpha = 0.36 \pm 0.008$ $\lambda = 1.64 \pm 0.021$ $k' = 3.5 \pm 0.4 \times 10^{-3}$/s $n = 20$ $d = 1100, 1300\ \mu m$	$\alpha = 0.42 \pm 0.012$# $\lambda = 1.58 \pm 0.032$ $k' = 3.4 \pm 0.3 \times 10^{-3}$/s $n = 24$ $d = 1500, 1700\ \mu m$
6–7	No data available	$\alpha = 0.31 \pm 0.019$ $\lambda = 1.67 \pm 0.044$ $k' = 5.0 \pm 1.5 \times 10^{-3}$/s $n = 6$ $d = 300\ \mu m$	$\alpha = 0.32 \pm 0.019$ $\lambda = 1.66 \pm 0.060$ $k' = 5.8 \pm 1.3 \times 10^{-3}$/s $n = 6$ $d = 500\ \mu m$	$\alpha = 0.30 \pm 0.009$* $\lambda = 1.65 \pm 0.057$ $k' = 7.3 \pm 1.8 \times 10^{-3}$/s $n = 11$ $d = 700, 900\ \mu m$	$\alpha = 0.34 \pm 0.012$* $\lambda = 1.68 \pm 0.067$ $k' = 8.4 \pm 1.7 \times 10^{-3}$/s $n = 12$ $d = 1100, 1300\ \mu m$	$\alpha = 0.42 \pm 0.012$# $\lambda = 1.64 \pm 0.080$ $k' = 8.6 \pm 1.7 \times 10^{-3}$/s $n = 5$ $d = 1500, 1700\ \mu m$
8–9	No data available	$\alpha = 0.29 \pm 0.011$* $\lambda = 1.61 \pm 0.025$ $k' = 3.1 \pm 0.7 \times 10^{-3}$/s $n = 6$ $d = 300\ \mu m$	$\alpha = 0.30 \pm 0.015$* $\lambda = 1.54 \pm 0.030$ $k' = 4.1 \pm 0.7 \times 10^{-3}$/s $n = 12$ $d = 500\ \mu m$	$\alpha = 0.27 \pm 0.014$# $\lambda = 1.49 \pm 0.033$ $k' = 4.7 \pm 0.5 \times 10^{-3}$/s $n = 18$ $d = 700, 900\ \mu m$	$\alpha = 0.32 \pm 0.010$ $\lambda = 1.55 \pm 0.020$ $k' = 5.0 \pm 0.5 \times 10^{-3}$/s $n = 27$ $d = 1100, 1300\ \mu m$	$\alpha = 0.40 \pm 0.020$# $\lambda = 1.54 \pm 0.014$ $k' = 3.5 \pm 0.7 \times 10^{-3}$/s $n = 14$ $d = 1500, 1700\ \mu m$
10–11	No data available	$\alpha = 0.26 \pm 0.020$ $\lambda = 1.59 \pm 0.050$ $k' = 8.4 \pm 2.8 \times 10^{-3}$/s $n = 9$ $d = 300\ \mu m$	$\alpha = 0.26 \pm 0.016$ $\lambda = 1.55 \pm 0.043$ $k' = 4.3 \pm 1.1 \times 10^{-3}$/s $n = 6$ $d = 700\ \mu m$	$\alpha = 0.25 \pm 0.009$* $\lambda = 1.52 \pm 0.017$ $k' = 4.7 \pm 0.3 \times 10^{-3}$/s $n = 27$ $d = 900, 1100\ \mu m$	$\alpha = 0.29 \pm 0.019$* $\lambda = 1.50 \pm 0.039$ $k' = 5.1 \pm 0.5 \times 10^{-3}$/s $n = 14$ $d = 1300, 1500\ \mu m$	$\alpha = 0.36 \pm 0.027$*# $\lambda = 1.52 \pm 0.024$ $k' = 5.0 \pm 0.6 \times 10^{-3}$/s $n = 19$ $d = 1700, 1900\ \mu m$
20–21	$\alpha = 0.19 \pm 0.003$# $\lambda = 1.35 \pm 0.019$ $k' = 5.4 \pm 0.5 \times 10^{-3}$/s $n = 5$ $d = 200\ \mu m$	$\alpha = 0.22 \pm 0.030$* $\lambda = 1.58 \pm 0.026$ $k' = 4.1 \pm 0.6 \times 10^{-3}$/s $n = 7$ $d = 500\ \mu m$	$\alpha = 0.22 \pm 0.005$* $\lambda = 1.61 \pm 0.020$ $k' = 4.6 \pm 0.5 \times 10^{-3}$/s $n = 8$ $d = 700\ \mu m$	$\alpha = 0.22 \pm 0.004$ $\lambda = 1.60 \pm 0.019$ $k' = 4.7 \pm 0.4 \times 10^{-3}$/s $n = 15$ $d = 900, 1100, 1300\ \mu m$	$\alpha = 0.23 \pm 0.005$* $\lambda = 1.50 \pm 0.016$ $k' = 3.2 \pm 0.3 \times 10^{-3}$/s $n = 14$ $d = 1700, 1900\ \mu m$	$\alpha = 0.19 \pm 0.005$*# $\lambda = 1.42 \pm 0.013$ $k' = 5.4 \pm 0.6 \times 10^{-3}$/s $n = 14$ $d = 2100, 2300\ \mu m$
90–120	$\alpha = 0.19 \pm 0.002$# $\lambda = 1.51 \pm 0.024$ $k' = 4.9 \pm 0.6 \times 10^{-3}$/s $n = 18$ $d = 200\ \mu m$	$\alpha = 0.20 \pm 0.004$# $\lambda = 1.63 \pm 0.032$ $k' = 5.6 \pm 0.4 \times 10^{-3}$/s $n = 10$ $d = 500\ \mu m$	$\alpha = 0.21 \pm 0.003$# $\lambda = 1.59 \pm 0.021$ $k' = 5.7 \pm 0.5 \times 10^{-3}$/s $n = 12$ $d = 700\ \mu m$	$\alpha = 0.22 \pm 0.003$ $\lambda = 1.62 \pm 0.012$ $k' = 6.3 \pm 0.4 \times 10^{-3}$/s $n = 24$ $d = 900, 1100, 1300\ \mu m$	$\alpha = 0.23 \pm 0.007$ $\lambda = 1.65 \pm 0.024$ $k' = 3.5 \pm 0.4 \times 10^{-3}$/s $n = 11$ $d = 1700, 1900\ \mu m$	$\alpha = 0.20 \pm 0.008$# $\lambda = 1.55 \pm 0.045$ $k' = 3.3 \pm 0.8 \times 10^{-3}$/s $n = 6$ $d = 2100, 2300\ \mu m$

α is ECS volume fraction, λ is ECS tortuosity, k' is nonspecific cellular uptake, n is number of measurements, d is depth to which the microelectrode array was lowered. For further details see Experimental Procedures. Statistical analysis of the differences between groups was evaluated by one-way ANOVA test. Significant differences ($P < 0.05$) are marked by *(vertical analysis) and by #(horizontal analysis).

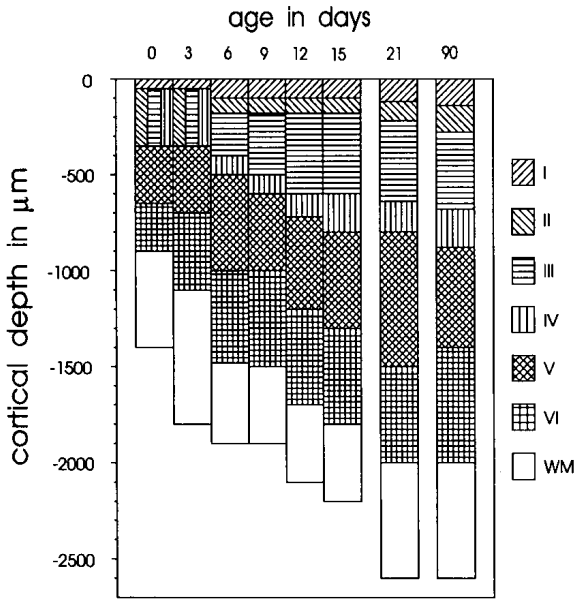

Fig. 3. Summary of anatomical data on distribution of layers in the postnatal rat cortex. The indicated regions represent the extent of the identified layers at different postnatal days. See Experimental Procedures and Table 1 for more details.

adult rats. The average α is between 0.36 and 0.41 in cortical layers III–VI and 0.46 in white matter. In a given animal the α obtained in a particular cortical layer was remarkably stable. In some animals ($n = 18$) the measurements were repeated with a second microelectrode array, with a different tip separation, however, the acquired α in the same cortical depth differed by less than 5%. These results show that in the early postnatal days, more than one third of the total nervous tissue volume is ECS.

The typical diffusion curves in layer VI of three-, 11-, 21- and 120-day-old rats are depicted in Fig. 4. Superimposed on each experimental curve is the theoretical curve derived from Eqn 1, using the three experimental parameters α, λ, and k′. While the α gradually decreased in all cortical layers and in white matter with age of animal, λ and k′ were not found to be significantly different (see Table 1).

Theoretical diffusion curves for the cortical layers IV, V, VI and for the subcortical white matter at postnatal days 2–120 are shown at Fig. 5. Diffusion curves for Fig. 5 were computed using Eqn 1 and the mean value of α, λ and k′ as stated for the respective layer and white matter in Table 1. It is evident that the curve of lowest amplitude occurs at the earliest age due primarily to the large α at this time. Increase in curve amplitude with maturation reflects the declining α during postnatal development.

The diffusion curves in gray and white matter of the individual five- and 120-day-old animals are depicted in Fig. 6. During postnatal days 2–11, α was highest in white matter and in deeper cortical layers than in more superficial ones, implying that the ECS

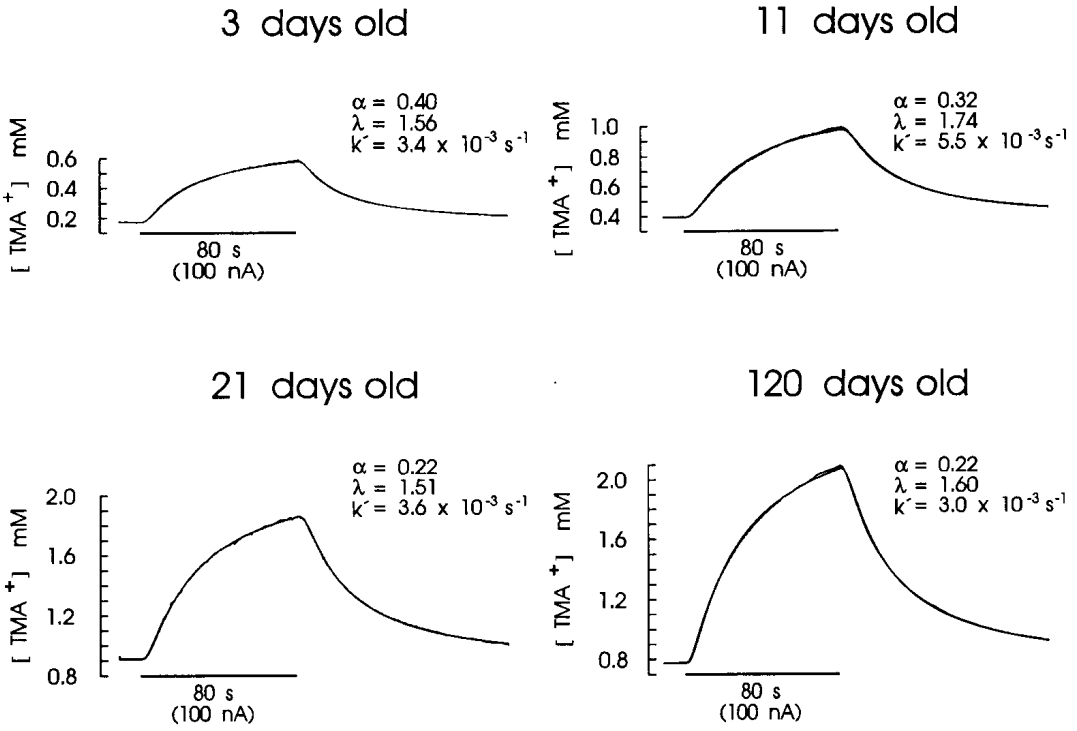

Fig. 4. Representative records obtained from layer VI of the cortex at different postnatal days. The separation between the ion-sensitive microelectrodes and iontophoresis electrodes tips and depth to which the arrays were lowered, respectively, were: three days, 158 μm, 1100 μm; 11 days, 167 μm, 1300 μm; 21 days, 178 μm, 1700 μm; 120 days, 165 μm, 1900 μm. The values of α, λ and k′ are shown with each record. Because of the differences in array spacing and value of k′, the amplitudes and shapes of the curves cannot be directly compared but another form of comparison is presented in Fig. 5.

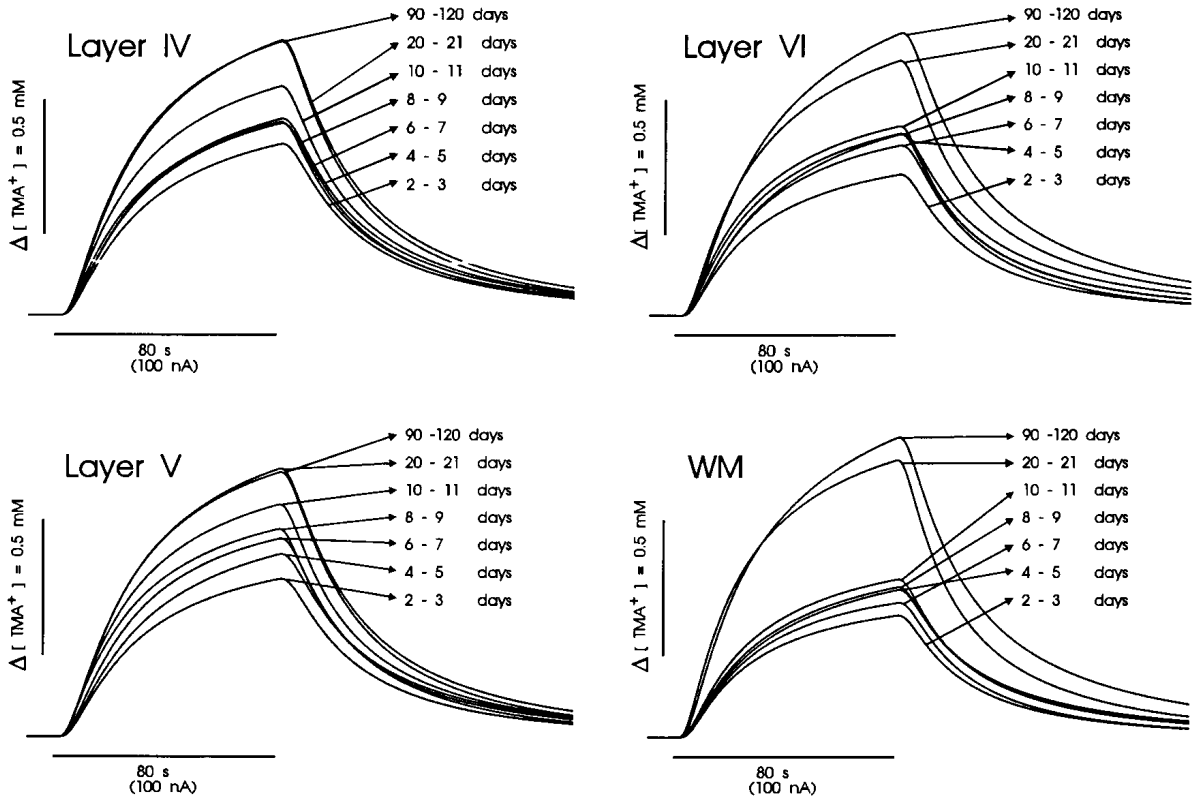

Fig. 5. Comparison of theoretical diffusion curves for layer IV, V, VI of the cortex and for the subcortical white matter (WM) at different postnatal days. Each curve was computed using Eqn 1 and the mean values of α, λ and k′ shown in Table 1 for layer IV, V and VI, respectively, as well as for white matter. To compare the curves we assumed constant spacing (175 μm), $D = 1.26 \times 10^{-5}$ cm^2/s and $n = 0.5$. Note that the curve of lowest amplitude occurs at the earliest age due primarily to the large volume fraction at that time. Increase in amplitude reflects the declining volume fraction with maturation.

volume fraction is larger in cortical layers V and VI and in white matter than in layers III and IV. During postnatal development the first significant ECS volume fraction decrease in α was found in cortical layers V and VI at postnatal days 6–7, in layers III and IV at days 8–9 and in white matter at days 10–11. A second significant decrease occurred in layers V and VI at days 10–11, in layers III and IV at days 20–21 and in white matter at days 20–21. A third significant decrease was found only in layer VI at days 20–21 (Table 1, Fig. 7). As it can be seen from Table 1 and Fig. 7 the α in the white matter significantly decreased later than that in gray matter. The α was still almost double the adult value at postnatal days 10–11, and the most dramatic decrease of the white matter ECS volume therefore occurred between postnatal days 10–11 and 20–21.

No significant difference in ECS volume fraction in any of the cortical layers, or in white matter, was found between animals aged 20–21 days and animals 90–120 days old (adults). In contrast to early postnatal days, the ECS volume fraction in white matter in rats 20–21 days old and older became significantly smaller than that in cortical layer VI (Table 1, Fig. 6). Moreover, in animals 20–21 days old the ECS volume fraction became significantly lower in cortical layer II than in layer VI. In adults of 90–120 days old, the α was lower in layers II, III and IV than in layer VI (Table 1).

There was no significant change in tortuosity λ and nonspecific uptake k′ during postnatal development in any of the cortical layers or in white matter.

In seven experiments (two rats aged eight to nine days, three rats aged 10–11 days and two adult rats aged 90 days) the microelectrodes passed through the white matter, as determined by comparison with measurements summarized in Fig. 3 and reached the ventriculus lateralis. The diffusion properties in this space were close to the diffusion properties of agar, i.e. $\alpha = 0.94 \pm 0.017$, $\lambda = 1.29 \pm 0.013$ and $k' = 1.5 \pm 0.17 \times 10^{-4}$/s ($n = 7$).

DISCUSSION

Extracellular space volume fraction and tetramethylammonium diffusion parameters

Electron microscopic study of brain extracellular spaces has been a controversial topic for the past 15 years. The narrow (150–200 Å wide) extracellular space that is visible in routine electron micrographs is now recognized to be largely an artifact of chemical fixation;[65] but even in these studies, the intercellular space was found to be much larger in the developing brain. It is apparent that the enlarged spaces shown

in some electron-microscopic studies were real but the estimated ECS volume fraction was most likely an error.

The rapid freezing used in our histology apparently preserved water and ion distribution more faithfully than chemical fixation does. Indeed we found good correlation between the microelectrodes' localization established by anatomical measurements and by changes in diffusion parameters recorded *in vivo*. In two- to 11-day-old rats the ECS volume fraction increased abruptly just when the electrode reached the white matter. Moreover, we often reached the lateral ventricle when we lowered microelectrode array just below white matter as determined by the measurements summarized in Figs 2 and 3.

Previous developmental analyses of ECS in the CNS with electron microscopy have been limited to small areas, mostly of neuropil,[8,9,11,12,18,43] and those with an indirect method using ECS markers have been confined to whole brains.[5,66] There have been no systematic studies to elucidate the overall developmental sequence of ECS and its distributional pattern within a specific region of the CNS.

Our data represent the first characterization of the diffusion properties of the developing brain, including the ECS volume fraction in defined small regions of the CNS. To date there was also no information available about diffusion parameters and size of the ECS in the white matter in either the developing or the adult brain. In considering the results of the white

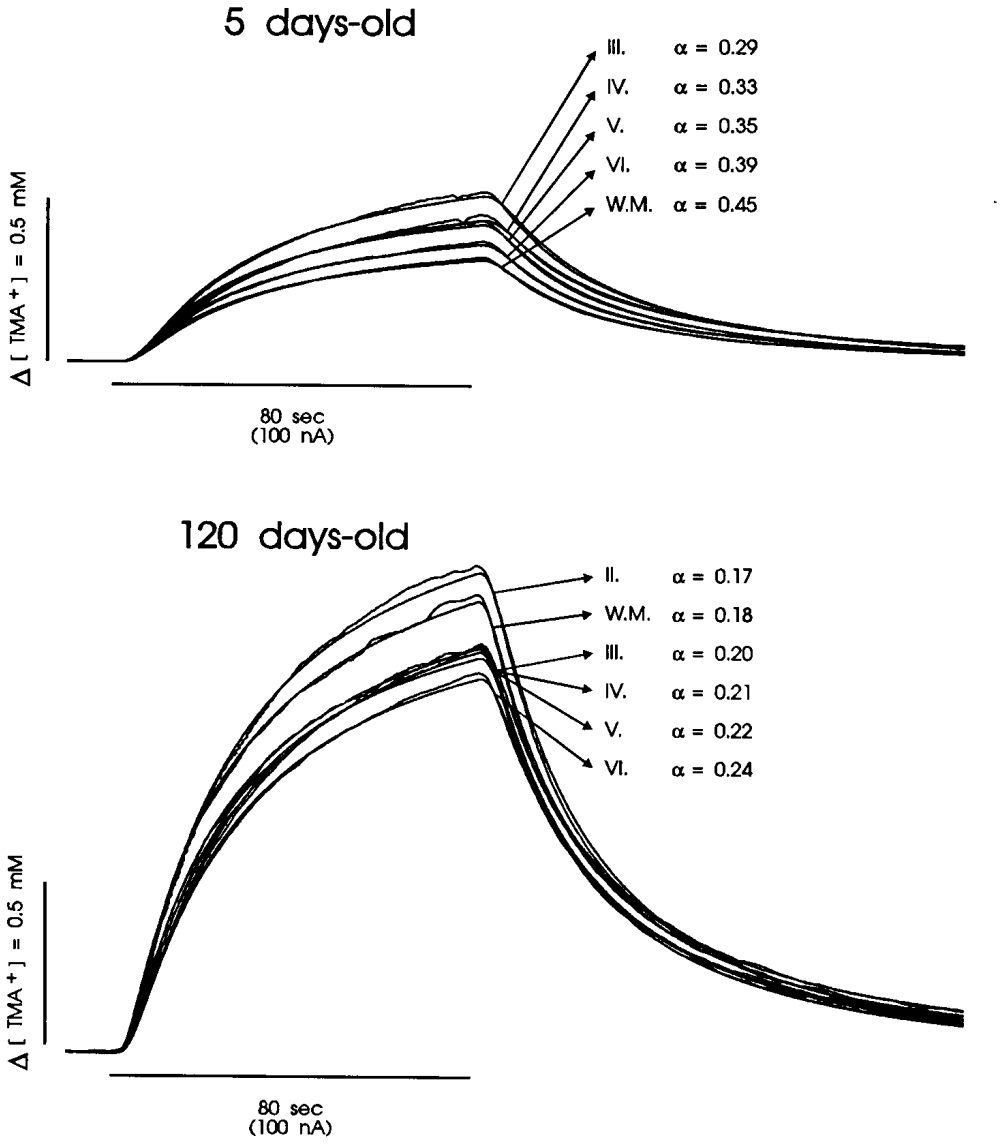

Fig. 6. Set of records in different layers from five- and 120-day-old cortex. The values of volume fraction (α) are shown on the figure. The values of tortuosity (λ), uptake (k') and depth to which the arrays were lowered, respectively, were in five-day-old cortex: layer III, 1.71, 4.5×10^{-3}/s, 300 μm; layer IV, 1.63, 4.0×10^{-3}/s, 900 μm; layer V, 1.67, 1.6×10^{-3}/s, 900 μm; layer VI, 1.62, 2.8×10^{-3}/s, 1300 μm; white matter, 1.62, 3.1×10^{-3}/s, 1500 μm; the array spacing was 158 μm. In 120-day-old cortex: layer II, 1.52, 5.0×10^{-3}/s, 300 μm; layer III, 1.48, 3.5×10^{-3}/s, 500 μm; layer IV, 1.55, 5.4×10^{-3}/s, 700 μm; layer V, 1.59, 3.6×10^{-3}/s, 900 μm; layer VI, 1.57, 4.0×10^{-3}/s, 1300 μm; white matter, 1.39, 1.6×10^{-3}/s, 2300 μm; the array spacing was 164 μm.

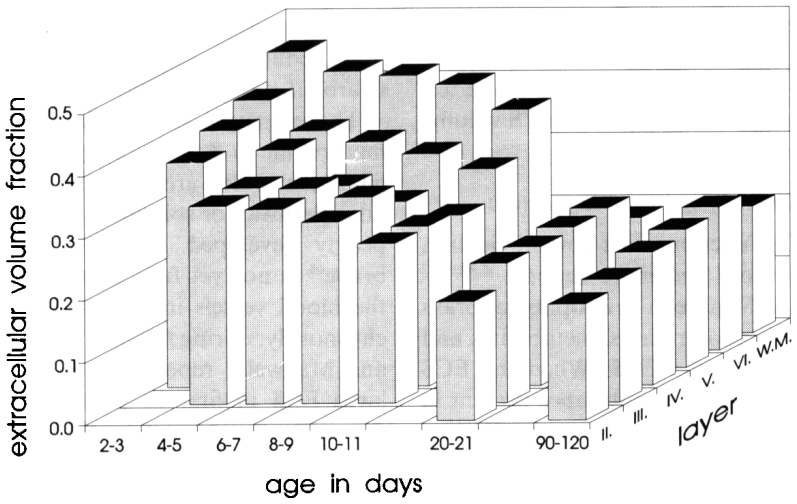

Fig. 7. Three-dimensional bar chart depicting the distribution of volume fraction as a function of age in postnatal days and layer. The figure is based on the data in Table 1. Note that the x-axis is non-continuous. The layers II and III were too small to make measurements at some early ages.

matter studies we note that white matter is anisotropic and this could affect the analysis of diffusion. To completely analyse the behaviour of the TMA^+ molecules, diffusion measurements would be required in two or three dimensions, depending on symmetry of white matter structure. In the experiments reported here the electrode array was aligned with the fibres of the white matter and the λ values associated with other electrode orientations could differ from that reported. If there are different λ values for different orientations then the calculation of α values from a set of measurments made in only one axis will be subject to systematic error. Uptake should not be affected, however. Finally, the relevance of anisotropy could change as the brain matures and fibre tracts become more defined. These conclusions are based on an unpublished study by Rice *et al.* Our results unequivocally show that the extracellular space volume fraction (α) in all cortical layers as well as in subcortical white matter is significantly higher in early postnatal days (two to 11 postnatal days) than in adult rats. However, no significant differences in tortuosity λ and nonspecific uptake k′ were detected during postnatal development either in different cortical layers or in white matter, suggesting that the tortuosity of the ECS matrix and the non-specific cellular uptake resemble that in mature tissue. This is not surprising since α and λ are independent parameters,[37] although given some additional structural constraints a relation could exist between them. λ is in a sense a measure of topology of the ECS, i.e. the connectivity, and this will not change if the connections are simply enlarged or narrowed. The λ could be changed if certain pathways through the ECS are either blocked off or opened up. Our results however seem to indicate that the connectivity does not significantly change with postnatal development, i.e. that large scale syncytia or extensive membrane appositions do not form or dissolve during the developmental process.

It is evident from our experiments that the diffusion parameters are not changing uniformly during postnatal development throughout the individual layers of the cortical gray matter and in white matter. The total thickness of the gray matter is almost doubled in first 15 postnatal days, as can be seen from Figs 2 and 3. This is a period of extensive growth and migration of neuronal elements. Caley and Maxwell[11] suggested that the presence of large extracellular spaces is associated with the period of extensive dendritic and axonal growth and their disappearance with the development of the complex cellular interrelationships.

Postnatal development of the rat brain is accomplished during the first 30 days of life.[1,16] Extensive gliogenesis occurs in gray matter during the first 14 postnatal days. Glial fibrillary acidic protein mRNA undergoes a two-step developmental expression. It increases between birth and day 15 (period of astrocytic proliferation) and then decreases until day 55 (period of astrocytic morphological differentiation).[48] The astrocytic proliferation therefore correlates well with time-course of the postnatal ECS volume decrease in gray matter (see Fig. 7). It is, however, evident that the first significant decrease of the white matter ECS volume occurs later. At postnatal days 10–11 the ECS volume fraction in white matter is still almost double that of white matter of 20-day-old animals and older. This suggests that α decreases rapidly during the extensive period of myelinization, which takes part in the second and particularly in the third postnatal week. As can also be seen from Fig. 2, the thickness of the white matter increases substantially from postnatal days 15–21. After postnatal day 21 the thickness of both the gray and white matter stays constant. It is, therefore, evident that the ratio between the intracellular and extracellular volume changes during the brain maturation and there is an increase of total brain volume, apparently due to the increase in the cell density, cell migration,

axonal growth, dendritic sprouting and glial cell maturation. The growth and maturation of the cortical gray matter, as well as subcortical white matter, is inversely related to the decrease of the ECS volume fraction.

Role of the extracellular space volume fraction

The idea that ECS functions as a communication channel is receiving more and more support.[35,40,56,57] The relatively large ECS space in developing rat brain may affect the accumulation of ions, metabolites and neuroactive substances in the ECS. When the ECS volume fraction diminishes, any substance present in or released to the ECS undergoes a corresponding increase in its concentration.[42,46] The diffusion will be governed by the value of α and λ, with the apparent diffusion coefficient given by D/λ^2, where D is the free diffusion coefficient. It has long been known from electron-microscopic studies that the developing nervous tissue has a larger ECS and greater abundance of the extracellular glycosaminoglycans and hyaluronate than the adult tissue[31] which might affect the movement of charged molecules. Our results show, however, that tortuosity and nonspecific TMA^+ uptake are not significantly changed in non-stimulated and normoxic developing cortical tissue. It remains to be shown whether these diffusion parameters differ under pathological conditions in the developing brain.

The relatively large ECS volume during development would have a drastic dilution effect on substances released from cells. The large activity-related ionic changes which occur during pathological events such as anoxia, seizures or spreading depression would be reduced as well as excessive accumulation of excitatory aminoacids, inhibitory transmitters, metabolic substrates related to those pathological states. Low ECS volume fraction is a prerequisite for a more marked change (shrinkage) during activity and elevation in $[K^+]_e$. This could be a reason for the increased vulnerability of the adult brain to cell damage after ischemia or hypoxia, epileptic seizures and spreading depression, which cause a rise in $[K^+]_e$, acidosis and ECS volume shrinkage.[28,42,47,60] Indeed, the relative susceptibility of the immature brain to anoxia, ischemia and seizures is smaller than in adult brain.

Even under physiological conditions, a decrease in the ECS volume fraction would lead to a larger rise in the interstitial concentration of transmitters, such as glutamate and glycine, and thus could lead to larger tonic activation of *N*-methyl-D-aspartate receptors, greater transient ionic changes particularly enhanced $[K^+]_e$ during cell firing, which affects neuronal excitability and synchronization. One of the mechanisms that could promote neuronal synchronization is the increase in $[K^+]_e$. Rising $[K^+]_e$ promotes interictal bursting and seizure activity in the hippocampal slice.[62] In small ECS volume the K^+ will be more concentrated during bursts than in large ECS during development. The persisting elevated $[K^+]_e$ could be important therefore for long-term neuronal synchronization.

The immature CNS is known to differ from the mature one in that vascularization is incomplete and glial cells, which are assumed to comprise a transcellular pathway of solutes and small molecules,[15,20] are poorly developed. The outer glial limiting membrane[68] is not yet fully established.[17] The growth of the blood vessels in rat cerebral cortex occurs synchronously, during the first 10 postnatal days.[11] Caley and Maxwell[11] report few patent blood vessels, but large ECS in first 10 postnatal days, while in the second 10 postnatal days the majority of the vessels develop patent lumina, the perivascular sheath of astrocyte end-feet and the large ECS size disappear. There may be an inverse relationship between the amount of ECS and the degree of vascularization; ECS may provide the major pathway for metabolites before blood vessels penetrate into the brain. On the other hand, diffusion could be effective for delivering soluble components to cells, with transport distances of the order of hundreds of micrometres and is likely to be an efficient form of transport before extensive growth of the neurites, dendrites, glial cells and prior to the development of vascularisation.

It is also likely that some aspects of the developmental process (e.g. guidance of migrating processes) depend on the existence of diffusion gradients in the ECS. The diffusion of peptides, hormones and growth factors, as well as drugs to which cell membranes are not easily permeable, would be facilitated in a larger ECS and slowed down in a smaller one. The access of hormones (e.g. oxytocin and vasopressin in neural lobe) to the capillaries could also be largely determined by the size and geometry of the ECS.[2] It is also evident that diffusion of Ca^{2+} in ECS could be changed during development. It has been shown that Ca^{2+} diffusion is influenced by the ECS size and the tortuosity of the tissue rather than other factors such as binding to extracellular charged sites or uptake.[38]

Role of glia in regulation of extracellular space volume

The first glial cells assigned to the cerebral cortex can be recognized morphologically around the time of birth in the rat.[7,10,22] Thereafter, there is a steady glial proliferation at least until 180 days postnatally.[21] Their relative number is especially high in the cerebral cortex.[6] Cell processes form expansions on to the surface of blood vessels, the so-called end-feet. Other processes extend to the surface of the CNS to form similar expansions that constitute the glial limiting membrane. The role of astrocytes during development is to guide migrating neurons[30,44] and influence the phenotypic expression of neuronal morphology[25,51] and to participate in synaptic re-organization.[49,63]

Maturation of a glial cell syncytium could contribute to ECS volume fraction decrease. The time course

of the postnatal decrease in ECS volume goes hand in hand with postnatal changes in ionic homeostasis. In early postnatal days, ionic and volume homeostasis is impaired, presumably due to incomplete gliogenesis. In the developing rat optic nerve,[45] in rat spinal cord,[24] in chick neostriatum[58] as well as in spinal cord when the gliogenesis is blocked by early postnatal X-irradiation[59] the K^+ and pH homeostasis is impaired, apparently due to insufficient glial cell function, e.g. insufficient membrane transport mechanisms, spatial buffering, gap junctions and low carbonic anhydrase activity.

Glial cells show dynamic changes in their volume during exposure to elevated K^+, changes of pCO_2, intracellular acidosis, non-isotonic media and neurotransmitters (for review, see Refs 3, 4, 26, 27, 67). The fact that there can be a certain level of tonic spontaneous activity in mature brain accompanied by extracellular ionic changes which would lead to tonic glial cell swelling, is also consistent with decrease of the ECS volume during gliogenesis. There is also evidence for glial cells swelling and ECS volume fraction shrinkage during neuronal activity in adult rat spinal cord,[53] while activity-dependent ECS shrinkage and ionic homeostasis are essentially absent in the neonatal rat optic nerve and spinal cord and become a robust phenomenon by the second week of life.[24,45] We can therefore assume that morphological and functional maturation of glial cells play an important role in the decrease of the ECS volume fraction during postnatal development.

REFERENCES

1. Arender A. T. and de Vellis J. (1989) Development of the nervous system. In *Basic Neurochemistry: Molecular, Cellular and Medical Aspects* (eds Siegel G. J., Agranoff B., Alberts R. N. and Nolinoff P.), pp. 479–504. Raven Press, New York.
2. Armstrong W. E., Tian M. and Reger J. F. (1991) Elevated extracellular potassium is associated with a reduced extracellular space in rat neural lobe *in vitro*. *J. Neurocytol.* **20,** 564–572.
3. Ballanyi K. and Grafe P. (1988) Cell volume regulation in the nervous system. *Renal Physiol. Biochem.* **3–5,** 142–157.
4. Ballanyi K., Grafe P., Serve G. and Schlue W.-R. (1990) Electrophysiological measurements of volume changes in leech neuropile glial cells. *Glia* **3,** 151–158.
5. Barlow C. F., Domek N. S., Goldberg M. A. and Roth L. J. (1961) Extracellular brain space measured by ^{35}S-sulfate. *Arch. Neurol.* **5,** 102–110.
6. Bass N. H., Hess H. H., Pope A. and Thalheimer C. (1971) Quantitative cytoarchitectonic distribution of neurons, glia and DNA in rat cerebral cortex. *J. comp. Neurol.* **143,** 481–490.
7. Berry N. and Rogers A. W. (1965) The migration of neuroblasts in the developing brain cortex. *J. Anat.* **99,** 691–709.
8. Bondareff W. (1967) An intercellular substance in rat cerebral cortex: submicroscopic distribution of ruthenium red. *Anat. Rec.* **157,** 527–536.
9. Bondareff W. and Pysh J. J. (1968) Distribution of extracellular space during postnatal maturation of rat cerebral cortex. *Anat. Rec.* **160,** 773–780.
10. Bruckner G., Mareš V. and Biesold D. (1976) Neurogenesis in the visual system of the rat. An autoradiographic investigation. *J. comp Neurol.* **166,** 245–256.
11. Caley D. M. and Maxwell D. S. (1970) Development of the blood vessels and extracellular spaces during postnatal maturation of rat cerebral cortex. *J. comp. Neurol.* **138,** 31–48.
12. Del Cerro M. P., Snider P. S. and Oster M. L. (1968) Evolution of the extracellular space in immature nervous tissue. *Experientia* **24,** 929–930.
13. Dietzel I., Heinemann U., Hofmeier G. and Lux H. D. (1980) Transient changes in the size of the extracellular space in the sensorimotor cortex of cats in relation to stimulus-induced changes in potassium concentration. *Expl Brain Res.* **40,** 432–439.
14. Dietzel I., Heinemann U. and Lux H. D. (1989) Relations between slow extracellular potential changes, glial potassium buffering, and electrolyte and cellular volume changes during neuronal hyperactivity in cat brain. *Glia* **2,** 25–44.
15. Dobbing J. (1963) The blood–brain barrier: some recent developments. *Guy's Hosp. Rep.* **112,** 267–286.
16. Eayrs J. T. and Goodhead G. (1959) Postnatal development of the cerebral cortex of the rat. *J. Anat.* **93,** 385.
17. Fujita S. (1965) An autoradiographic study on the origin and fate of the subpial glioblast in the embryonic chick spinal cord. *J. comp. Neurol.* **124,** 51–60.
18. Hannah R. S. and Nathaniel E. J. H. (1974) The postnatal development of blood vessels in the substantia gelatinosa of rat cervical cord—an ultrastructural study. *Anat. Rec.* **178,** 691–710.
19. Hansen A. (1985) Effect of anoxia on ion distribution in the brain. *Physiol. Rev.* **65,** 101–148.
20. Henn F. A., Haljamae H. and Hamberger A. (1972) Glial cell function: active control of extracellular K^+ concentration. *Brain Res.* **43,** 437–443.
21. Heumann D., Leuba G. and Rabinowicz T. (1978) Postnatal development of the mouse cerebral neocortex. IV. Evolution of the total cortical volume of the population of neurons and glial cells. *J. Hirnforsch.* **19,** 385–393.
22. Hicks S. P. and D'Amato C. J. (1968) Cell migrations to the isocortex in the rat. *Anat. Rec.* **160,** 619–634.
23. Hounsgaard J. and Nicholson C. (1983) Potassium accumulation around individual Purkinje cells in cerebellar slices from the guinea pig. *J. Physiol., Lond.* **340,** 359–388.
24. Jendelová P. and Syková E. (1991) Role of glia in K^+ and pH homeostasis in the neonatal rat spinal cord. *Glia* **4,** 56–63.
25. Johnson M. I., Higgins D. and Ard N. D. (1989) Astrocytes induce dendritic development in cultured sympathetic neurons. *Devl Brain Res.* **47,** 289–292.
26. Kempski O. (1986) Cell swelling mechanisms in brain. In *Mechanisms of Secondary Brain Damage* (eds Baethmann A., Go K. G. and Unerberg A.), pp. 203–220. Plenum Publishing Corporation, New York.
27. Kimelberg H. K. and Frangakis N. V. (1986) Volume regulation in primary astrocyte cultures. *Adv. Biosci.* **61,** 177–186.

28. Lehmenkühler A., Caspers H. and Kersting U. (1985) Relations between DC potentials, extracellular ion activities and extracellular volume fraction in the cerebral cortex with changes in pCO_2. In *Ion Measurements in Physiology and Medicine* (eds Kessler M., Harrison D. K. and Hopfer J.) pp. 199–205. Springer, Berlin.
29. Lehmenkühler A., Svoboda J., Zilles K. and Syková E. (1992) Extracellular volume fraction in the neocortex and in the subjacent white matter of the developing rat brain. In *Rhythmogenesis in Neurons and Networks* (eds Elsner N. and Richter D. W.), p. 618 Thieme, Stuttgart.
30. Levitt P. and Rakic P. (1980) Immunoperoxidase localization of glial fibrillary acidic protein in radial glial cells and astrocytes of the developing rhesus monkey brain. *J. comp. Neurol.* **193,** 815–840.
31. Margolis R. U., Aquino M. M., Klinger J. A., Ripellino J. A. and Margolis R. K. (1986) Structure and localization of nervous tissue proteoglycans. *Ann. N.Y. Acad. Sci.* **481,** 46–52.
32. McBain C. J., Traynelis S. F. and Dingledine R. (1990) Regional variation of extracellular space in the hippocampus. *Science* **249,** 674–677.
33. Merker B. (1983) Silver staining of cell bodies by means of physical development. *J. Neurosci. Meth.* **9,** 235–241.
34. Nicholson C. (1979) Brain cell microenvironment as a communication channel. In *The Neurosciences Fourth Study Program* (eds Schmidt F. O. and Worden F. G.), pp. 457–476. MIT Press, Cambridge, MA.
35. Nicholson C. (1992) Measurement of extracellular space. In *Practical Electrophysiological Methods: A Guide for* In Vitro *Studies in Vertebrate Neurobiology* (eds Kettenmann H. and Grantyn R.), pp. 367–372. John Wiley, New York.
36. Nicholson C. (1992) Quantitative analysis of extracellular space using the method of TMA^+ iontophoresis and the issue of TMA^+ uptake. *Can. J. Physiol. Pharmac.* **70,** 5314–5322.
37. Nicholson C. and Phillips J. M. (1981) Ion diffusion modified by tortuosity and volume fraction in the extracellular microenvironment of the rat cerebellum. *J. Physiol., Lond.* **321,** 225–257.
38. Nicholson C. and Rice M. (1986) The migration of substances in the neuronal microenvironment. *Ann. N.Y. Acad. Sci.* **481,** 55–66.
39. Nicholson C. and Rice M. E. (1988) Use of ion-selective microelectrodes and voltametric microsensors to study brain cell microenvironment. In *Neuromethods: The Neuronal Microenvironment* (eds Boulton A. A., Baker G. B. and Walz W.), Vol. 9, pp. 247–361. Humana Press, New York.
40. Nicholson C. and Rice M. E. (1991) Diffusion of ions and transmitters in the brain cell microenvironment. In *Volume Transmission in the Brain, Novel Mechanisms for Neural Transmission* (eds Fuxe K. and Agnati L. F.), pp. 279–294. Raven Press, New York.
41. Paxinos G., Tork I., Tesott L. H. and Valentino K. L. (1991) *Atlas of the Developing Rat Brain.* Academic Press, San Diego.
42. Phillips J. M. and Nicholson C. (1979) Anion permeability in spreading depression investigated with ion selective microelectrodes. *Brain Res.* **173,** 567–571.
43. Pysh J. J. (1969) The development of the extracellular space in neonatal rat inferior colliculus: an electron microscopic study. *Am. J Anat.* **124,** 411–430.
44. Rakic P. (1971) Neuron-glia relationship during granule cell migration in developing cerebellar cortex. A Golgi and electron microscopic study in *Maccacus rhesus. J. comp. Neurol.* **141,** 283–312.
45. Ransom B. R., Yamate C. L. and Connors B. W. (1985) Activity dependent shrinkage of extracellular space in rat optic nerve: A developmental study. *J. Neurosci.* **5,** 532–535.
46. Rice M. E. and Nicholson C. (1987) Interstitial ascorbate in turtle brain is modulated by release and extracellular volume change. *J. Neurochem.* **49,** 1096–1104.
47. Rice M. and Nicholson C. (1991) Diffusion characteristics and extracellular volume fraction during normoxia and hypoxia in slices of rat neostriatum. *J. Neurophysiol.* **65,** 264–272.
48. Riol H., Fages C. and Tardy M. (1992) Transcriptional regulation of glial fibrillary acidic protein (GFAP)-mRNA expression during postnatal development of mouse brain. *J. Neurosci. Res.* **32,** 79–85.
49. Ronevi L. O. (1978) Origin of the glial processes responsible for the spontaneous postnatal phagocytosis of boutons on cat spinal motoneurons. *Cell Tiss. Res.* **189,** 203–217.
50. Rosen A. S. and Andrew R. D. (1990) Osmotic effects upon excitability in rat neocortical slices. *Neuroscience* **38,** 579–590.
51. Rousselet A. A., Autillo-Touati D. Arand and Prochiantz A. (1990) *In vitro* regulation of neuronal morphogenesis and polarity by astrocyte-derived factors. *Devl Biol.* **137,** 33–45.
52. Sumi S. M. (1969) The extracellular space in the developing rat brain: its variation with changes in osmolarity of the fixative, method of fixation and maturation. *J. ultrastruct. Res.* **29,** 398–425.
53. Svoboda J. and Syková E. (1991) Extracellular space volume changes in the rat spinal cord produced by nerve stimulation and peripheral injury. *Brain Res.* **560,** 216–224.
54. Svoboda J., Lehmenkühler A. and Syková E. (1992) Extracellular volume fraction in the developing neocortex. *Pflügers Arch.* **420,** Suppl. 1, R18.
55. Syková E. (1987) Modulation of spinal cord transmission by changes in extracellular K^+ activity and extracellular volume. *Can. J. Physiol. Pharmac.* **65,** 1058–1066.
56. Syková E. (1991) Activity-related ionic and volume changes in neuronal microenvironment. In *Volume Transmission in the Brain: Novel Mechanisms for Neural Transmission* (eds Fuxe K. and Agnati L. F.), pp. 217–336. Raven Press, New York.
57. Syková E. (1992) Ionic and volume changes in the microenvironment of nerve and receptor cells. *Progress in Sensory Physiology* 13, pp. 1–167 Springer, Heidelberg.
58. Syková E., Jendelová P., Svoboda J., Sedman G. and Ng K. T. (1990) Activity-related rise in extracellular potassium concentration in the brain of 1–3-day-old chicks. *Brain Res. Bull.* **24,** 569–575.
59. Syková E., Jendelová P., Šimonová Z. and Chvátal A. (1992) K^+ and pH homeostasis in the developing rat spinal cord is impaired by early postnatal X-irradiation. *Brain Res.* **594,** 19–30.
60. Syková E., Svoboda J. and Polák J. (1992) Extracellular space volume and tortuosity changes in the rat spinal cord evoked by afferent stimulation, anoxia and EAE. In *Abstracts of the 15th Annual Meeting of the European Neuroscience Association Munich, Eur. J. Neurosci., Suppl.* 5, p. 233.
61. Torack R. M. (1980) Ultrastructural studies of subependymal extracellular spaces in adult and neonatal rat brain. *Histochemistry* **68,** 297–307.

62. Traynelis S. F. and Dingledine R. (1989) Role of extracellular space in hyperosmotic suppression of potassium-induced electrographic seizures. *J. Neurophysiol.* **61,** 927–938.
63. Tweedle C. D. and Hutton G. I. (1984) Ultrastructural changes in rat hypothalamic neurosecretory cells and their associated glia during minimal dehydratation and rehydratation. *Cell Tiss. Res.* **181,** 59–72.
64. Van Harreveld A. (1972) The extracellular space in the vertebrate central nervous system. In *The Structure and Function of Nervous Tissue* (ed. Bourne G. H.), Vol. IV, pp. 447–511. Academic Press, New York.
65. Van Harreveld A. and Khattab F. I. (1968) Perfusion fixation with glutaraldehyde and post-fixation with osmium tetroxide for electron microscopy. *J. Cell Sci.* **3,** 579–594.
66. Vernadakis A. and Woodbury D. M. (1965) Cellular and extracellular spaces in developing rat brain. *Arch. Neurol.* **12,** 284–293.
67. Walz W. (1987) Swelling and potassium uptake in cultured astrocytes. *Can. J. Physiol. Pharmac.* **65,** 1051–1057.
68. Weigert C. M. (1890) Bemerkungen über das Neurogliagerust des menschlichen Centralnervensystem. *Anat. Anz.* **5,** 543–551.
69. Zilles K. (1985) *The Cortex of the Rat. A Stereotaxic Atlas.* Springer, Berlin.

(*Accepted* 16 *February* 1993)